Conducting the Temperature-Dependent Conformational Change of Macrocyclic Compounds to the Lattice Dilation of Quantum Dots for Achieving an Ultrasensitive Nanothermometer

Ding Zhou,[†] Min Lin,[†] Xun Liu,[†] Jing Li,[†] Zhaolai Chen,[†] Dong Yao,[†] Haizhu Sun,[‡] Hao Zhang,[†,*] and Bai Yang[†]

[†]State Key Laboratory of Supramolecular Structure and Materials, College of Chemistry, Jilin University, Changchun 130012, People's Republic of China and [‡]College of Chemistry, Northeast Normal University, Changchun 130024, People's Republic of China

ABSTRACT We report a ligand decoration strategy to enlarge the lattice dilation of quantum dots (QDs), which greatly enhances the characteristic sensitivity of a QD-based thermometer. Upon a multiple covalent linkage of macrocyclic compounds with QDs, for example, thiolated cyclodextrin (CD) and CdTe, the conformation-related torsional force of CD is conducted to the inner lattice of CdTe under altered temperature. The combination of the lattice expansion/contraction of CdTe and the stress from CD conformation change greatly enhances the shifts of both UV—vis absorption and photoluminescence (PL) spectra, thus improving the temperature sensitivity. As an example, β-CD-decorated CdTe QDs exhibit the 0.28 nm shift of the spectra per degree centigrade (0.28 nm/°C), 2.4-fold higher than those of monothiol-ligand-decorated QDs.

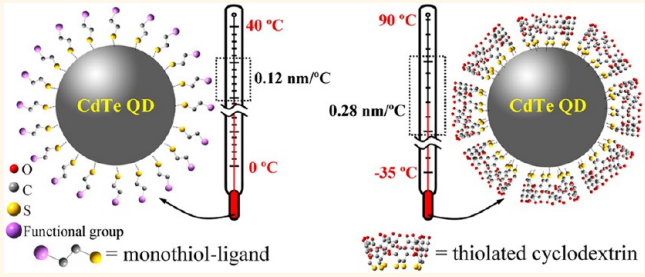

KEYWORDS: conformation change · cyclodextrins · lattice dilation · quantum dots · thermometer

Temperature is a critical thermodynamic parameter in many biological and biotechnological processes.[1,2] State-of-the-art control of the organism temperature enables development of novel theranostic techniques, which leads to the current challenge of measuring the local temperature and temperature gradient in the nanoscale regime.[3−9] This issue is considered to be overcome by virtue of the temperature-dependent color change of luminescent probes, which simultaneously possess the advantages of high temporal and spatial resolutions, low cost, and facility. Among various probes, semiconductor nanoparticles (NPs), also known as quantum dots (QDs), are competitive candidates because of good photostability,[4−6,10−14] tunable luminescence,[15−19] and easy surface decoration.[20−23] However, determined by the intrinsic properties of QDs, including temperature-dependent lattice dilation,[24,25] energy gap,[24,26] and electron—phonon coupling,[25,26] their characteristic sensitivity has been concluded to be ~0.12 nm/°C by numerous experimental investigations and theoretical calculations.[25−33] The limited sensitivity makes the current device design mainly based on the fabrication of multicolor and fluorescence resonance energy transfer-based nanostructures.[34−42] Still, the enhancement of the characteristic sensitivity of basic QD building blocks is an ongoing challenge.

Jaque *et al.* have predicted that the thermal sensitivity of QDs may relate to the surface tensile stress, attributed to the large surface-to-volume ratios of nanometer-sized particles.[43] However, it is difficult to introduce enough stress by the conventional

* Address correspondence to hao_zhang@jlu.edu.cn.

Received for review November 22, 2012 and accepted February 7, 2013.

Published online February 12, 2013
10.1021/nn305423p

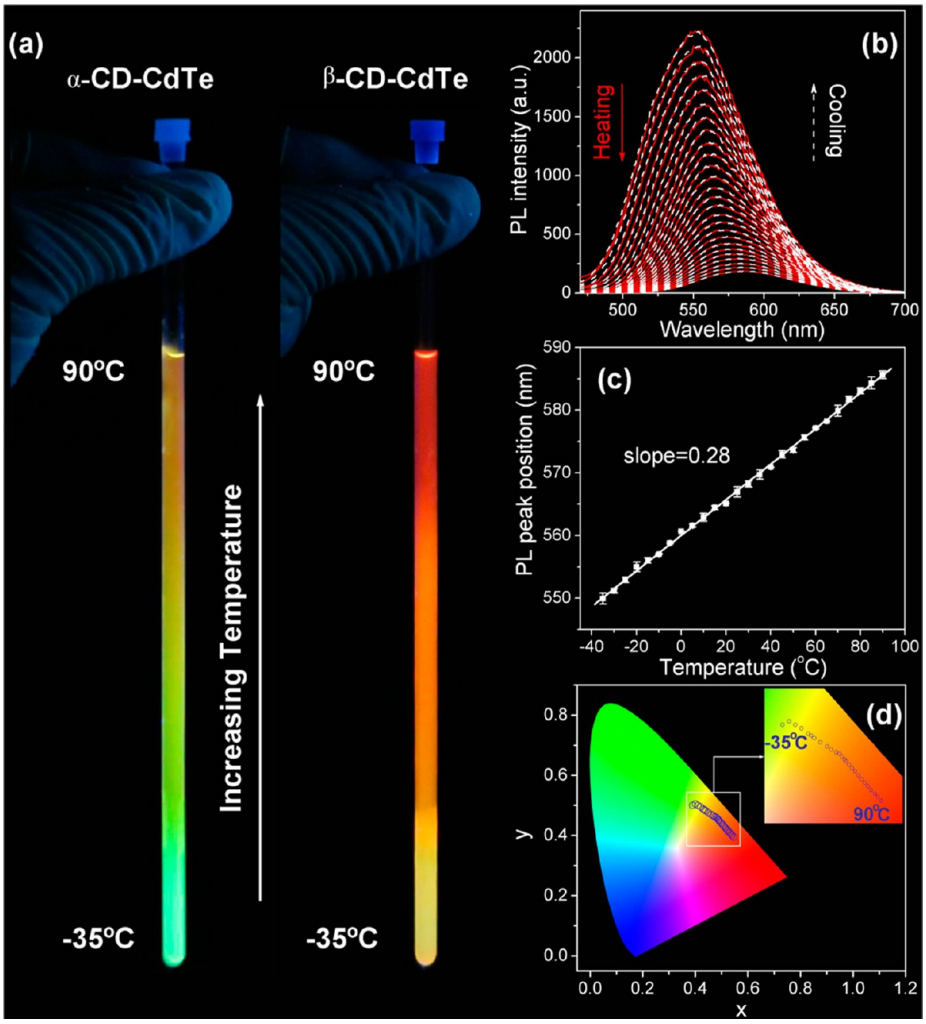

Figure 1. (a) Gradient fluorescence of α-CD- and β-CD-decorated CdTe QD aqueous solution in quartz tubes. (b) Series of fluorescence spectra of β-CD-decorated CdTe QDs that are measured with the increase of temperature from −35 to 90 °C at a step of 5 °C (red solid), and that from 90 to −35 °C (white dash). (c) Temperature-dependent fluorescence peak position of β-CD-decorated CdTe QDs. (d) CIE chromaticity diagram showing the temperature dependence of the (*x*,*y*) color coordinates of β-CD-decorated CdTe QDs.

surface decoration techniques. Surface decoration of QDs with organic ligands is widely employed to tune the luminescence,[44,45] solubility,[46−49] stability,[50] chirality,[51−53] and conjugation behavior.[15−17] Such strategy is carried out by affecting the surface atoms of QDs. To enlarge the inner lattice expansion/contraction of QDs, the key for determining the characteristic sensitivity of QDs, a strong and directional force is necessary. In this scenario, macrocyclic compounds are potentially available because of the multiple binding with QDs and the abundant conformers under environmental variations.[54] As a well-documented macrocyclic compound, cyclodextrin (CD) consists of six or more α-(l→4)-linked glucopyranose rings.[55−58] The primary hydroxyls of each pyranose ring can rotate around the C−O bonds under altered temperature, which has been mentioned in much of the literature (Supporting Information Figure S1).[55−58] If the considerable torsional force generated by the conformational change is conducted to the lattice dilation of QDs, the sensitivity of a QD-based thermometer is expected to be improved. In this paper, thiolated CDs are decorated on aqueous CdTe QDs to conduct the temperature-dependent conformational change of CD to the lattice dilation of CdTe, which significantly enhances the characteristic sensitivity to 0.28 nm/°C (Figure 1).

RESULTS AND DISCUSSION

In our experiments, aqueous CdTe QDs, decorated with per-6-thio-α-cyclodextrin (α-CD) and per-7-thio-β-cyclodextrin (β-CD), are synthesized through a room-temperature N_2H_4-promoted strategy.[59] The as-synthesized QDs are purified by centrifugation for various characterizations (Figure 2). Under transmission electron microscopy (TEM), the as-synthesized QDs are quasi-spherical particles, consistent with the previously reported aqueous CdTe.[59] The high-resolution TEM images indicate that the lattice parameters of

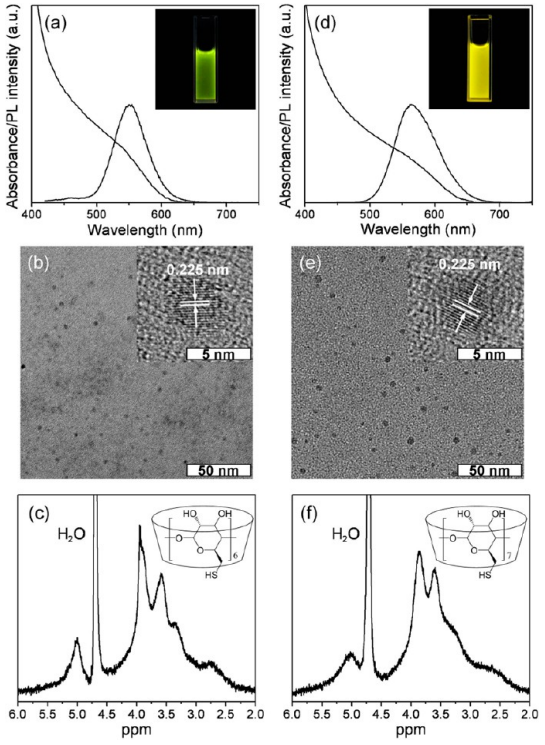

Figure 2. UV−vis absorption and PL spectra of α-CD- (a) and β-CD-decorated (d) CdTe QDs. Insets: corresponding PL images of the aqueous solutions of QDs. TEM images of α-CD- (b) and β-CD-decorated (e) CdTe QDs. Insets: HRTEM images. ^{1}H NMR of α-CD- (c) and β-CD-decorated (f) CdTe QDs. Insets: illustrated molecular structures of α-CD and β-CD.

CdTe QDs fit well to the zinc blende structure of the bulk CdTe crystal. The ^{1}H NMR spectra of the CD-decorated CdTe QDs show sharp intense peaks corresponding to D_2O molecules plus broad peaks that are assigned to immobilized thiolated CDs. This is consistent with the previous report about CD-decorated Au nanoparticles.[60] Because the excessive CDs have been removed by QD purification, the NMR spectra confirm that the CdTe QDs are modified with thiolated CDs. In comparison to the CdTe QDs decorated with monothiol ligands, such as 3-mercaptopropionic acid (MPA), thioglycolic acid (TGA), 2-mercaptoethylamine (MA), and 1-thioglycerol (TG), α-CD- and β-CD-decorated ones exhibit the temperature-dependent shift of both UV−vis absorption and photoluminescence (PL) spectra with high sensitivity and repeatability in a broadened range (Figures 1, 3, 4, and S2). Note that, though the N_2H_4 in the solution does not affect the sensitivity (Figure S3), it significantly lowers the freezing point of water to below −35 °C. So, the reservation of N_2H_4 can broaden the measure range of the thermometer down to −35 °C (Figure 1a). As shown in Figures 1b and S2a, a series of PL spectra of α-CD- and β-CD-decorated CdTe QDs are measured with the increase of temperature from −35 to 90 °C at a step of 5 °C and recorded both forward and reverse to ensure the reproducibility. For β-CD-decorated CdTe QDs, the PL peak position and temperature indicate a good linear relationship (Figure 1c), which fits well to the function of $T = 3.52\lambda_{max} - 1971.9$ with a correlation coefficient of 0.9989, where λ_{max} is the PL peak position (nm) and T is the system temperature (°C). The wavelength shift per degree centigrade is calculated to be 0.28 nm, which can be measured using a modern fluorescence spectrometer by showing the accuracy better than 1 °C.[8] Similar to β-CD-decorated QDs, the α-CD-decorated ones also exhibit the sensitivity of 0.24 nm/°C (Figure S2b). These results are among the highest thermal resolution of the QD thermometers on the basis of the shift of PL peak position.[39,40] Although several QD systems have shown greater sensitivity, they are dual-emitting mode thermometers by monitoring the intensity ratio of two PL peaks.[34,41] Such strategy only enhances the sensitivity in a limited temperature range, whereas measuring the shift of the PL peak permits linear observation in a broadened range. Figure 1d shows the color change of the PL in the Commission Internationale de L'Eclairage (CIE) 1931 chromaticity diagram from −35 to 90 °C. The system color shifts between yellow and salmon pink, which is consistent with the apparent PL of the QD solution (Figure 1a).

As mentioned above, β-CD-decorated QDs indicate the sensitivity of 0.28 nm/°C, whereas the sensitivities of MPA-, TGA-, MA-, and TG-decorated QDs are all around 0.12 nm/°C, which is independent of the experimental variables, such as the concentration and size of QDs (Figure 3c,d). According to the empirical Varshni-type function, the sensitivity of a II−VI semiconductor should be a constant, which is defined as $d\lambda/dT$ (Figure S4).[61] It is true for monothiol-ligand-decorated QDs (Figure 3c,d) because the adsorption/desorption equilibrium of monothiol ligands is rather dynamic.[62] The conformational change has less effect on the inner lattice of QDs (Figure S5a). However, the multiple thiol−Cd binding of β-CD with QDs greatly suppresses the dynamic equilibrium of β-CD adsorption/desorption, making the thiol−QD bonds intact after QD formation (Figure S5b). Even one thiol−Cd bond is liable to break by thiol desorption, and this thiol will remain on the surface of the QD owing to the limitation of the rigid CD macrocycle. As a result, the torsional force generated by the conformational change of β-CD under altered temperature can be released neither by β-CD desorption nor by the molecular rotation, but conducted to the inner lattice of QDs. The combination of the lattice expansion/contraction of the QD and that from β-CD stress greatly enhances the sensitivity. In our experiment, CdTe QDs are also decorated with 6-monodeoxy-6-monothio-β-cyclodextrin, which is a monothiolated β-CD. The QDs exhibit the sensitivity of 0.12 nm/°C, completely the same as other monothiol-ligand-decorated CdTe QDs (Figure 3c). Our results are

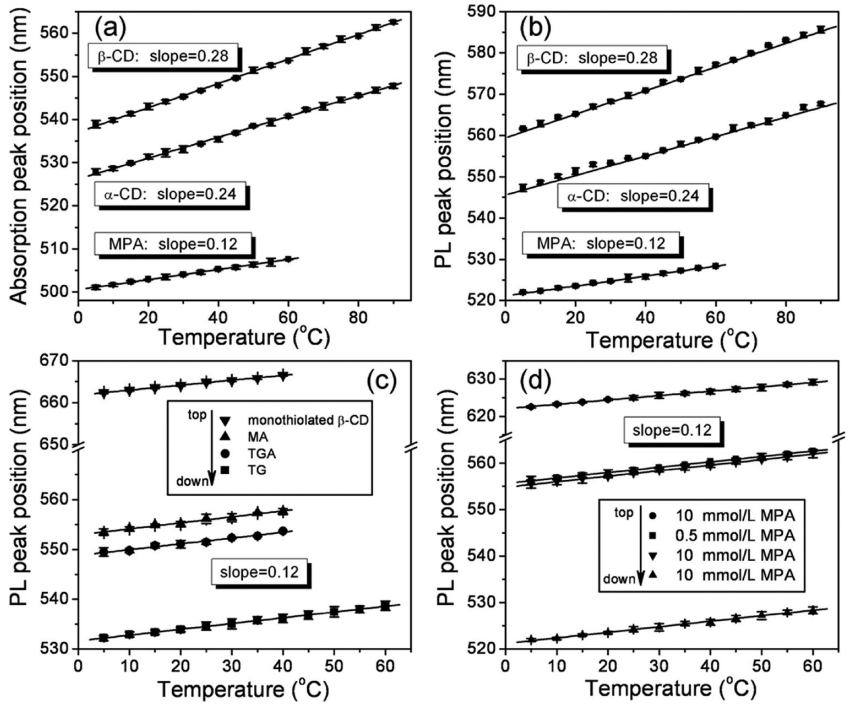

Figure 3. Shift of the peak positions of UV−vis absorption (a) and PL (b) spectra of β-CD-, α-CD-, and MPA-decorated CdTe QDs *versus* temperature. The slopes measured from the absorption and PL spectra are almost the same. (c) Influence of various monothiol ligands on the slopes. The concentrations of QDs are 10 mmol/L, referring to the concentration of Cd^{2+}. Monothiolated β-CD-, MA-, and TGA-decorated QDs are not measured above 40 °C because of the irreversible thermal growth. (d) Effect of the concentration and size of MPA-decorated CdTe QDs on the slopes. The QDs with two concentrations of 10 and 0.5 mmol/L and three emission colors of green, yellow, and red are investigated. The diameter of green, yellow, and red QDs is 2.3, 3.1, and 4.2 nm, respectively.

consistent with the previous prediction that the thermal sensitivity of QDs should relate to the surface tensile stress.[43] Only polydentate CDs generate enough stress to enhance the sensitivity, whereas monothiol ligands do not. This clearly proves that the multiple binding of CDs with QDs is the key for conducting the CD conformation change to the QD lattice dilation.

Figure 5 illustrates the conformational change of β-CD between two different temperatures. When temperature increases, it does not obviously alter the conformational freedom of macro-ring shapes and each pyranose ring of β-CD. Also, the conformation of the secondary hydroxyls is not considerably changed. These are attributed to the homodromic and intermolecular hydrogen bonds between the neighboring secondary hydroxyls in different pyranose rings, reducing the conformational freedom of macro-ring shapes and pyranose rings. However, the torsional angle (ω) of the primary sulfhydryls, which directly link with QDs, exhibits larger conformational freedom because of less limitation of rotational freedom. With increasing temperature, the primary sulfhydryls will leave from the cone cavity of β-CD, arising to the torsional force to enlarge the lattice dilation of QDs. Note that the stress to the lattice of QDs from the CD conformational change is very strong, which can be estimated by combining the pressure coefficient of the excitonic energy gap of CdTe. The contribution from β-CD conformational change on the lattice dilation is 0.16 nm/°C (Figure S6), attributed to the influence of external pressure on the excitonic energy gap. The pressure coefficient of the excitonic energy gap of CdTe is about 7.9×10^{-2} eV/GPa.[63,64] Thus, the generated pressure per degree centigrade is calculated to be 8.4 MPa (*i.e.*, 8.4 pN/nm^2), comparable to that of azobenzene conformational changes.[65] This consideration is further confirmed by studying the characteristic sensitivity of CdSe QDs (Figure 6). The sensitivity of MPA- and β-CD-decorated CdSe is 0.11 and 0.21 nm/°C, respectively. The lower sensitivity, in comparison to CdTe, is attributed to the lower pressure coefficient of the excitonic energy gap of CdSe, which is 5.0×10^{-2} eV/GPa (Table 1).[63,64] The different pressure coefficient means that, under the same external force, the spectral shift of CdTe should be 1.58 times larger than that of CdSe. In experiment, the influence of the conformational change of β-CD induces the CdTe spectral shift 1.6 times larger than that of CdSe, consistent with the anticipation.

Similarly, the contribution from α-CD conformational change is also strong, which is equal to the expansion coefficient of CdTe. The smaller contribution of α-CD is understandable in terms of the structural difference of α-CD and β-CD that, in comparison to β-CD, α-CD lacks one glucopyranose ring and therefore one sulfhydryl. It leads to weaker stress toward QDs

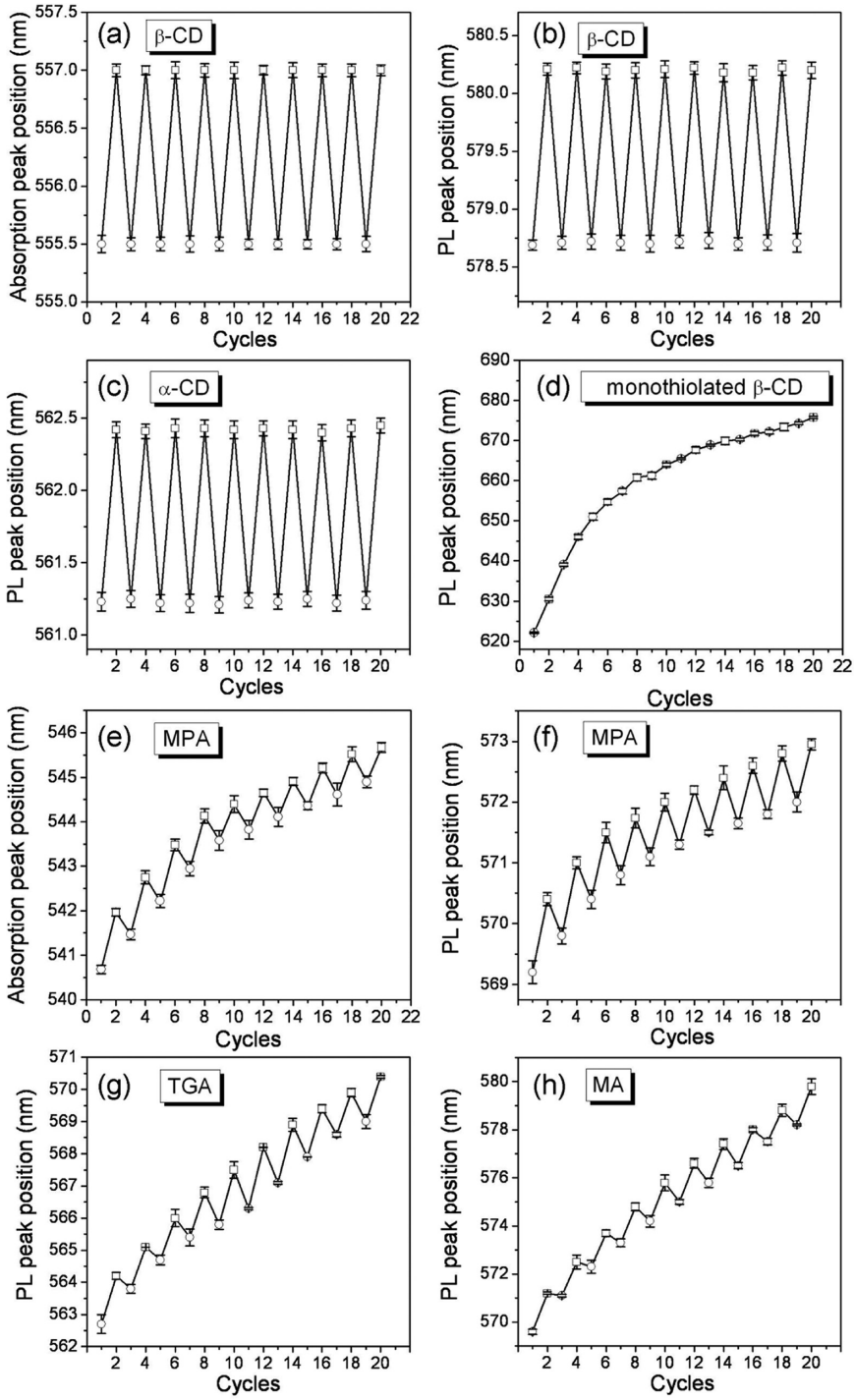

Figure 4. Variation of the peak positions of the UV−vis absorption (a,e) and PL (b−d,f−h) spectra of the CdTe QDs decorated with β-CD (a,b), α-CD (c), monothiolated β-CD (d), MPA (e,f), TGA (g), and MA (h) during the temperature recycle between 65 (circle) and 70 (square) °C. In each recycle, the PL spectra are measured after storing the QD solution for 20 min.

and the lowered sensitivity of 0.24 nm/°C. This result in return proves that the sensitivity enhancement results from the conformational change of CD. To further confirm the consideration, CdTe QDs are co-decorated using β-CD and TG with a molar ratio of 1:1, referring to sulfhydryls. As shown in Figure S7, the sensitivity becomes 0.17 nm/°C between β-CD-decorated QDs and TG-decorated ones. The decrease of β-CD ratio is reasonable to lower the contribution from the conformational change, making the sensitivity close to the inherent lattice thermal expansion coefficient of CdTe.

Note that the effect of CD conformation on the variation of Cd−Te bond length is very tiny, but it is enough for enhancing the sensitivity. In bulk CdTe, 1 °C variation only alters the lattice of 4.7×10^{-6}, corresponding to the energy band gap change of

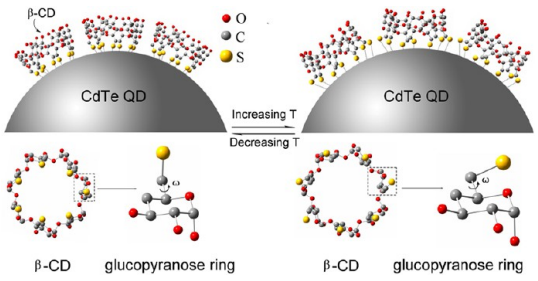

Figure 5. Scheme showing the conformation change of β-CD with temperature variation. For better visibility, the hydrogen atoms are not shown.

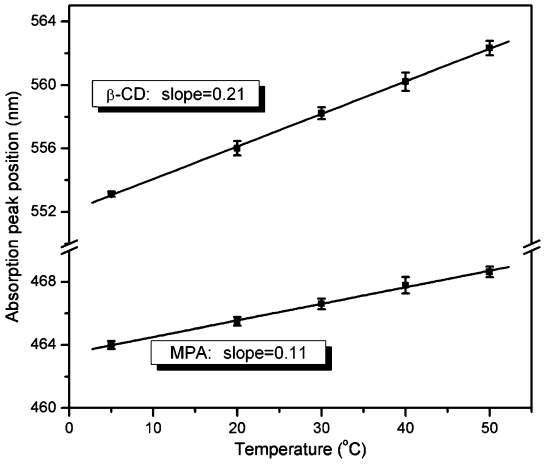

Figure 6. Shift of the peak positions of UV–vis absorption spectra of β-CD- and MPA-decorated CdSe QDs *versus* temperature.

TABLE 1. Pressure Coefficient of the Excitonic Energy Gap of Some Common Semiconductors Obtained from Reference 64

substance	dE_g/dp (10^{-2} eV/GPa)
CdTe	7.9
CdSe	5.0
CdS	4.2
ZnTe	7.0
ZnSe	7.0
ZnS	6.3

3.5×10^{-4} eV.[64] In the case of QDs, such alteration leads to the shift of PL spectra of about 0.1 nm. Besides, for 3 nm CdTe QDs, about 35% atoms locate on the surface and link with thiolated CDs, making the influence of CD conformation more significant.[43,66,67] In our experiment, the tensile stress generated from CD conformation change shows a larger effect on the QDs with smaller size owing to the larger surface-to-volume ratio, for example, 3.0 nm β-CD-decorated CdTe QDs exhibit higher sensitivity than that of the 3.9 nm ones (Table 2). It should be emphasized that such size effect is only observed for CD-decorated QDs (Figure S8c,f) because strong tensile stress is generated by CD conformational change. Monothiol ligands cannot generate such stress, thus making the sensitivity independent of the QD size in our investigated size range (Figure 3d). Therefore, it is concluded that the torsional force generated by the conformational change of CDs can greatly enhance the characteristic sensitivity of QDs, which leads to larger effect for the QDs with smaller size.

In addition, the temperature-dependent PL shift of QDs may contribute from three aspects, including the alteration of the lattice of materials, quantum-confined energy from QD size variation, and the electron–phonon coupling interaction.[68] The presence of the torsional force from CD conformational change directly enlarges the expansion/contraction of QDs, relating both to the lattice and size of QDs (Figure 3). However, the influence on the lattice plays the key role because the intrinsic lattice thermal expansion coefficient of II–VI semiconductor materials is small, and the subsequent QD size variation under altered temperature is also small. As a result, the contribution from QD quantum-confined energy on the temperature sensitivity is not serious. Moreover, the contribution from electron–phonon interactions is negligible. In the current system, the strength of electron–phonon coupling can be evaluated by the Stokes shift of QDs, which is small and in particular unchanged with the variation of QD size (Figure 3a,b). It means that the electron–phonon coupling has little contribution to the sensitivity enhancement. In all, it can be safely concluded that the enhancement of the characteristic sensitivity of CD-decorated CdTe QDs results from the CD-directed lattice dilation, including primary material lattice expansion/contraction and secondary quantum-confined energy variation of QDs.

Spectral stability is important in utilizing QD-based nanothermometers. In our investigation, β-CD is a polydentate ligand, which endows the as-synthesized QDs with high size stability and subsequent spectral stability (Figures 7 and S9). Even after 6 month storage at room temperature, no PL change is observed (Figure 7a). The stability of β-CD-decorated CdTe QDs in glutathione solution is also studied because cells have 5–10 mM glutathione as well as other free thiols. After aging β-CD-decorated CdTe QDs in 10 mM glutathione solution for 24 h, the PL spectra are nearly identical (Figure S10a), showing good stability in the simulated thiol surrounding. In comparison, monothiol-ligand-decorated CdTe QDs are unstable in glutathione solution (Figure S10b). This experiment confirms the potential of CD-decorated QD sensor in biological systems. More importantly, the QDs also exhibit high size stability under elevated temperature. Even maintaining the QD solutions at 90 °C for 4 h, no absorption and PL spectral shift are observed (Figures 7b,c and S9), showing the unchanged QD size, whereas obvious size increase of monothiol-ligand-decorated QDs is found at the temperature over 60 °C. To demonstrate the repeatability of a QD-based

TABLE 2. Summaries of the Experimental and Expected Thermal Sensitivities, Working Range, Stability of Different Ligand-Decorated CdTe QDs

mercapto ligands	sensitivity (nm/°C)	working range (°C)	stability of the QDs[b]	expected sensitivity (nm/°C)
TGA	0.12	0—40	stable	0.11
TG	0.12	0—60	stable	0.11
MA	0.12	0—40	moderate	0.11
MPA	0.12	0—60	stable	0.11
thiolated α-CD	0.24	−35—90	very stable	*c*
thiolated β-CD	0.28	−35—90	very stable	*c*
monothiolated β-CD	0.12	0—35	stable	0.11
thiolated β-CD (3.0 nm QDs transferred from organic media)[a]	0.17	0—60	stable	*d*
thiolated β-CD (3.9 nm QDs transferred from organic media)[a]	0.14	0—60	stable	*d*

[a] In revealing the size effect, the CdTe QDs are foremost synthesized in organic media and transferred to water *via* the ligand exchange using β-CD. Other QDs are directly synthesized in water using different mercapto ligands. [b] The stability of monothiol-ligand-decorated CdTe QDs is obtained from ref 46. The stability of α-CD- and β-CD-decorated CdTe QDs is estimated by comparing with the monothiol-ligand-decorated ones. [c] The expected thermal sensitivity of β-CD-decorated CdTe QDs should be larger than that of α-CD-decorated ones. [d] Though the thermal sensitivity of β-CD-decorated CdTe QDs with different sizes cannot be expected, the smaller QDs possess larger sensitivities due to larger surface-to-volume ratio.

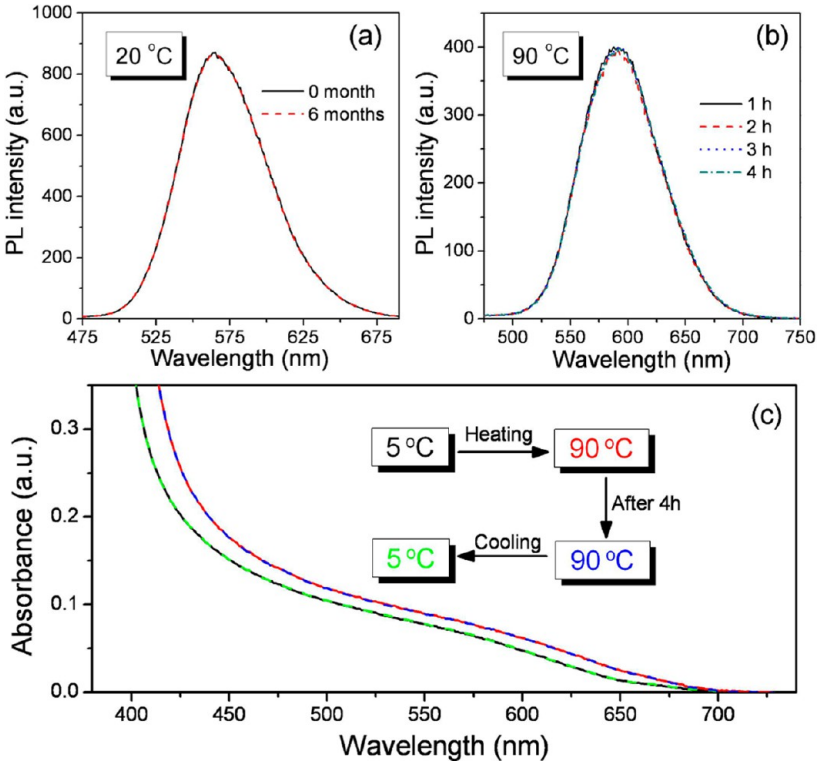

Figure 7. PL spectra of β-CD-decorated CdTe QDs are measured by storing at (a) 20 and (b) 90 °C for different duration. (c) UV—vis absorption spectra of β-CD-decorated CdTe QDs that are measured at 5 °C (black solid), 90 °C (red solid), 90 °C for 4 h (blue dash), and finally cooled to 5 °C (green dash).

thermometer, the absorption and PL spectra of α-CD-, β-CD-, TGA-, MA-, and MPA-decorated QDs are measured with the recycles between 65 and 70 °C for 20 times (Figure 4). In each recycle, the PL spectra are measured after a 20 min thermal equilibration. Because the test temperature is higher than the critical growth temperature of TGA-, MA-, and MPA-decorated CdTe QDs, the spontaneous growth of QDs and subsequent PL red shift are inevitable (Figure 4d—h). This is essentially attributed to the weaker binding of monothiol ligands with QDs, leading to a dynamic equilibrium of ligand adsorption and desorption.[62] As a result, the spontaneous growth of QDs occurs if the temperature is higher than the critical growth temperature, whereas no spectra shift is found for α-CD- and β-CD-decorated QDs after 20 recycles (Figure 4a—c) because of the relatively high critical growth temperature (Figures 7 and S9). As mentioned above, N_2H_4 lowers the freezing point of water, making the thermometer potentially usable at −35 °C (Figure 1a). However, only α-CD- and

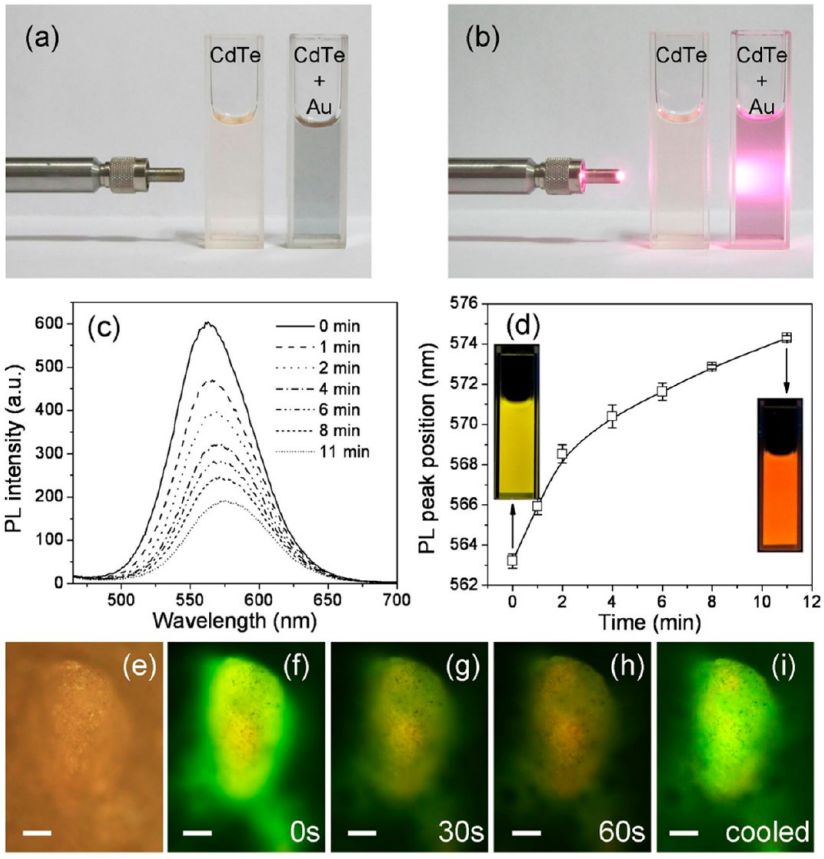

Figure 8. β-CD-decorated CdTe QDs as the nanothermometer to exhibit the photothermal behavior of PPy-enveloped branched Au NPs. Optical photographs of CdTe and Au−CdTe mixture without (a) and with (b) 808 nm irradiation. The dependence of the fluorescence spectra (c) and the shifts of peak positions (d) on the irradiation duration. Insets: fluorescent images of Au−CdTe mixture before and after 11 min irradiation. (e−i) Temperature maps of Au−CdTe film. Optical photograph (e) and the film with (f) 0, (g) 30, and (h) 60 s irradiation, after which the film is cooled to room temperature (i). Scale bar: 20 μm. The laser power density is 3 W/cm^2.

β-CD-decorated QDs are workable because N_2H_4 strongly promotes the growth of monothiol-ligand-decorated QDs.[59] Thus, the working range of the thermometers from most monothiol-ligand-decorated QDs is limited between 0 and 40 °C, whereas the range of α-CD- and β-CD-decorated QDs is −35 to 90 °C (Table 2).

The current strategy is also workable for high-quality QDs synthesized in high-boiling-point organic solvents, such as CdSe, CdTe, and CdSe/ZnS QDs (Figures S8 and S11). These hydrophobic QDs are decorated with MPA or β-CD *via* ligand exchange and transferred from organic media to water.[69] Similar to aqueous synthesized QDs, these QDs also exhibit ligand-dependent thermal sensitivities, though the values of sensitivity are not completely consistent (Table 2). The disparity is attributed to the impossibility of anchoring all seven mercapto groups of each β-CD with QDs during the ligand exchange in the presence of a large excess of ligands[69] and the complex core/shell structure of CdSe/ZnS QDs.[31] This is also the reason that we mainly employ aqueous synthesized QDs as nanothermometers.

The QD-based thermometer is applicable to monitor the temperature variation in microscale. β-CD-decorated CdTe QDs are mixed with polypyrrole (PPy)-enveloped Au nanoflowers and irradiated by an 808 nm laser to achieve temperature mapping (Figure 8). In this context, the heating source is PPy-enveloped Au nanoflowers. By adjusting the size of Au nanoflowers and the thickness of the PPy shell, the composite nanoflowers possess strong plasmon resonance absorption at 808 nm (Figure S12 and Table S1), thus efficiently converting the 808 nm irradiation into heat energy by virtue of photothermal effect.[70] In comparison, β-CD-decorated CdTe QDs cannot absorb 808 nm irradiation (Figure S13), only acting as the imaging agents. In the mixture of PPy-enveloped Au nanoflowers and β-CD-decorated CdTe QDs, the former strongly absorb the irradiation and convert to heat under an 808 nm laser irradiation (Figure 8b), thus rapidly raising the temperature over 50 °C. The temperature variation is clearly mapped by β-CD-decorated CdTe QDs, leading to the PL color alteration from yellow to orange (Figure 8c,d). Note that, for the nanothermometers from most monothiol-ligand-decorated QDs, the ceiling temperature is below 40 °C. Only CD-decorated QDs permit the mapping with high repeatability and accuracy (Figure 4). Figure 8e−i exhibits the microscale

PL mapping of the film composed of β-CD-decorated CdTe and PPy-enveloped Au under 808 nm irradiation. With prolonged irradiation, the PL turns from green, yellow, to orange, representing the temperature increase. When the film is cooled to the initial temperature, the PL returns to green. In comparison to the most recent work using CdSe QDs to measure the temperature change from 20 to 60 °C,[71] the CD-decorated CdTe possesses two improvements at least. First, the thermal sensitivity of the CdSe QDs is only 0.1 nm/°C, lower than that of the CD-decorated CdTe QDs (0.28 nm/°C). In the investigated temperature range (20−60 °C), the PL of CD-decorated CdTe QDs shifts 11.2 nm, much higher than the 4 nm shift of CdSe QDs. The temperature change is easier to observe with the naked eye. Second, CD-decorated CdTe QDs can be employed in a broad temperature range (−35 to 90 °C), whereas most non-CD-decorated QDs cannot avoid spontaneous growth over 60 °C as nanothermometers. Because of the good PL mapping behavior, CD-decorated QDs will be alternative candidates for further design and construction of nanothermometers.

CONCLUSIONS

In summary, the torsional force generated from the temperature-dependent conformational change of macrocyclic compounds was applied to enhance the sensitivity of a QD-based thermometer. The linkage of thiolated CD with aqueous CdTe QDs enables one to conduct this torsional force to the lattice dilation of QDs, thus dramatically enhancing the sensitivity to 0.28 nm/°C, 2.4-fold higher than those of monothiol-ligand-decorated QDs. Besides, the strong stabilization from thiolated CD suppressed the size alteration of QDs both in the presence of N_2H_4 and under elevated temperature, thus significantly broadening the application scope of the nanothermometer from −35 to 90 °C. Because CD-decorated QDs can monitor the temperature change in microscale with high sensitivity and repeatability, such a nanothermometer is potentially applicable in developing novel biomedical techniques.

METHODS

Materials. Tellurium powder (~200 mesh, 99.8%), 3-mercaptopropionic acid (MPA, 99+%), thioglycolic acid (TGA, 98%), 1-thioglycerol (TG, 98%), and 2-mercaptoethylamine (MA, 98%) were purchased from Aldrich. $NaBH_4$ (96%), Na_2TeO_3 (98+%), $CdCl_2$ (99%), and $N_2H_4\cdot H_2O$ (85%) were commercially available products and used as received. Per-6-thio-α-cyclodextrin (α-CD) and per-7-thio-β-cyclodextrin (β-CD) were synthesized according to the procedure described in the previous publication.[59]

Preparation of α-CD- and β-CD-Decorated CdTe and CdSe QDs. α-CD- and β-CD-decorated CdTe QDs were prepared in aqueous solution according to our previous work.[59] Typically, 2 mL of 100 mM $CdCl_2$ was placed in a conical flask first, then 32.4 mL of water, 70 mg of α-CD or β-CD, 2 mL of 20 mM Na_2TeO_3, 50 mg of $NaBH_4$, and 45.6 mL of 85% $N_2H_4\cdot H_2O$ were added in turn. The concentration of QDs was 2.5 mM referring to Cd^{2+}, and the molar ratio of Cd^{2+}/CD/TeO_3^{2-}/$NaBH_4$/$N_2H_4\cdot H_2O$ was 1:0.3:0.2:6.7:4000. β-CD-decorated CdSe QDs were synthesized *via* a similar method, except using NaHSe rather than TeO_3^{2-}. The QD solution was purified by adding 2-propanol and centrifuging. For NMR characterization, the precipitates were redissolved in D_2O.

Preparation of Aqueous CdTe and CdSe QDs Decorated with Monothiol Ligands. MPA-decorated CdTe QDs were prepared by injecting freshly prepared NaHTe solution into N_2-saturated $CdCl_2$ aqueous solution at pH 9.5 in the presence of MPA. The concentration of the precursors was 10 or 0.5 mM with reference to the concentration of Cd^{2+}, whereas the molar ratio of Cd^{2+}/MPA/HTe^- was 1:2.0:0.2. The precursors were then subjected to a reflux which controlled the growth of CdTe QDs. Following a similar procedure, CdTe QDs stabilized by TGA, MA, and TG and CdSe QDs stabilized by MPA were prepared. The QDs were purified by adding 2-propanol to the QD solution and centrifuging for further characterization.

Surface Decoration of the CdSe, CdTe, and CdSe/ZnS QDs That Are Foremost Synthesized in Organic Media. The CdSe, CdTe, and CdSe/ZnS QDs were synthesized in high-boiling-point organic solvents according to the previous publications.[72−74] Different thiol ligands, typically MPA and β-CD, were decorated on these QDs *via* ligand exchange, which transferred the QDs from organic media to water.[69] For example, the as-synthesized oleic acid (OA)-stabilized CdSe QDs in 1-octadecene were cooled to ~30−50 °C and precipitated by adding chloroform and methanol. After centrifugation, the supernatant was decanted, and the precipitate was dissolved in chloroform with the concentration of 20 mM. Then, 400 μL of MPA was added into 1 mL of the aforementioned solution with the Cd^{2+}/MPA molar ratio of 1:50. The solution was shaken for 20 min with sonication, which became turbid gradually due to the exchange of OA by MPA. The precipitate was isolated by centrifugation and dissolved in pH >10 deionized water. The excess MPA was further removed by washing the precipitate with chloroform and centrifuging to obtain MPA-decorated CdSe QDs. Through a similar method, CdSe QDs were decorated with β-CD, except using 0.2 mL of dimethylformamide as the solvent to dissolve 70 mg of β-CD. Note that a large excess of β-CD must be added to ensure a successful ligand exchange, at least 10 times higher than that employed in the aqueous synthesis of QDs. Following a similar procedure, CdTe and CdSe/ZnS QDs were decorated with MPA and β-CD.

Characterization. UV−visible absorption spectra were obtained using a Lambda 800 UV−vis spectrophotometer. Fluorescence spectroscopy was performed with a Shimadzu RF-5301 PC spectrophotometer. The excitation wavelength was 400 nm. Transmission electron microscopy (TEM) was conducted using a Hitachi H-800 electron microscope at an acceleration voltage of 200 kV with a CCD camera. High-resolution TEM (HRTEM) imaging was implemented by a JEM-2100F electron microscope at 300 kV. ^{1}H NMR was recorded on a Bruker Ultra Shield 500 MHz spectrometer in D_2O with tetramethylsilane as an internal standard. An Olympus BX-51 fluorescence microscope was used to examine the micrometer-scale temperature maps. The color of light was identified by the CIE (Commission Internationale de L'Eclairage 1931) colorimetry system. Any color could be described by the chromaticity (x,y) coordinates on the CIE diagram. Three means were adopted to ensure the accuracy of the measured temperature. First, a low constant temperature trough, whose accuracy is ±1 °C, is used to keep the exact temperature. Second, each measurement is taken three times at a given temperature following a 10 min equilibration period. Last, the average value is used for ensuring the accuracy, though the three values are very much in agreement.

Conflict of Interest: The authors declare no competing financial interest.

Acknowledgment. This work was supported by the 973 Program of China (2012CB933802, 2009CB939701), NSFC (21174051, 91123031, 21221063), and the Special Project from MOST of China.

Supporting Information Available: Schematic illustration of the temperature-dependent conformation change of one glucopyranose ring, theoretical analysis of the characteristic sensitivity of QD thermometer, and the experimental results of ligand-dependent sensitivity and stability of QDs. This material is available free of charge *via* the Internet at http://pubs.acs.org.

REFERENCES AND NOTES

1. Clausen, T.; Van Hardeveld, C.; Everts, M. E. Significance of Cation Transport in Control of Energy Metabolism and Thermogenesis. *Physiol. Rev.* **1991**, *71*, 733–774.
2. Narberhaus, F.; Waldminghaus, T.; Chowdhury, S. RNA Thermometers. *FEMS Microbiol. Rev.* **2006**, *30*, 3–16.
3. Li, S.; Zhang, K.; Yang, J. M.; Lin, L. W.; Yang, H. Single Quantum Dots as Local Temperature Markers. *Nano Lett.* **2007**, *7*, 3102–3105.
4. Lee, J.; Kotov, N. A. Thermometer Design at the Nanoscale. *Nano Today* **2007**, *2*, 48–51.
5. Fischer, L. H.; Harms, G. S.; Wolfbeis, O. S. Upconverting Nanoparticles for Nanoscale Thermometry. *Angew. Chem., Int. Ed.* **2011**, *50*, 4546–4551.
6. Walker, G. W.; Sundar, V. C.; Rudzinski, C. M.; Wun, A. W.; Bawendi, M. G.; Nocera, D. G. Quantum-Dot Optical Temperature Probes. *Appl. Phys. Lett.* **2003**, *83*, 3555–3557.
7. Brites, C. D. S.; Lima, P. P.; Silva, N. J. O.; Millán, A.; Amaral, V. S.; Palacio, F.; Carlos, L. D. A Luminescent Molecular Thermometer for Long-Term Absolute Temperature Measurements at the Nanoscale. *Adv. Mater.* **2010**, *22*, 4499–4504.
8. Feng, J.; Tian, K. J.; Hu, D. H.; Wang, S. Q.; Li, S. Y.; Zeng, Y.; Li, Y.; Yang, G. Q. A Triarylboron-Based Fluorescent Thermometer: Sensitive over a Wide Temperature Range. *Angew. Chem., Int. Ed.* **2011**, *50*, 8072–8076.
9. Ke, G. L.; Wang, C. M.; Ge, Y.; Zheng, N. F.; Zhu, Z.; Yang, C. J. L-DNA Molecular Beacon: A Safe, Stable, and Accurate Intracellular Nano-Thermometer for Temperature Sensing in Living Cells. *J. Am. Chem. Soc.* **2012**, *134*, 18908–18911.
10. Wang, S. P.; Westcott, S.; Chen, W. Nanoparticle Luminescence Thermometry. *J. Phys. Chem. B* **2002**, *106*, 11203–11209.
11. Chan, W. C. W.; Nie, S. M. Quantum Dot Bioconjugates for Ultrasensitive Nonisotopic Detection. *Science* **1998**, *281*, 2016–2018.
12. Tang, Z. Y.; Zhang, Z. L.; Wang, Y.; Glotzer, S. C.; Kotov, N. A. Self-Assembly of CdTe Nanocrystals into Free-Floating Sheets. *Science* **2006**, *314*, 274–278.
13. Peng, X. G.; Manna, L.; Yang, W. D.; Wickham, J.; Scher, E.; Kadavanich, A.; Alivisatos, A. P. Shape Control of CdSe Nanocrystals. *Nature* **2000**, *404*, 59–61.
14. Mokari, T.; Rothenberg, E.; Popov, I.; Costi, R.; Banin, U. Selective Growth of Metal Tips onto Semiconductor Quantum Rods and Tetrapods. *Science* **2004**, *304*, 1787–1790.
15. Dubertret, B.; Skourides, P.; Norris, D. J.; Noireaux, V.; Brivanlou, A. H.; Libchaber, A. *In Vivo* Imaging of Quantum Dots Encapsulated in Phospholipid Micelles. *Science* **2002**, *298*, 1759–1762.
16. Whaley, S. R.; English, D. S.; Hu, E. L.; Barbara, P. F.; Belcher, A. M. Selection of Peptides with Semiconductor Binding Specificity for Directed Nanocrystal Assembly. *Nature* **2000**, *405*, 665–668.
17. Medintz, I. L.; Uyeda, H. T.; Goldman, E. R.; Mattoussi, H. Quantum Dot Bioconjugates for Imaging, Labelling and Sensing. *Nat. Mater.* **2005**, *4*, 435–446.
18. Rajh, T.; Mićić, O. I.; Nozik, A. J. Synthesis and Characterization of Surface-Modified Colloidal CdTe Quantum Dots. *J. Phys. Chem.* **1993**, *97*, 11999–12003.
19. Bao, H. F.; Wang, E. K.; Dong, S. J. One-Pot Synthesis of CdTe Nanocrystals and Shape Control of Luminescent CdTe-Cystine Nanocomposites. *Small* **2006**, *2*, 476–480.
20. Cao, Y. W.; Banin, U. Growth and Properties of Semiconductor Core/Shell Nanocrystals with InAs Cores. *J. Am. Chem. Soc.* **2000**, *122*, 9692–9702.
21. Nedeljković, J. M.; Mićić, O. I.; Ahrenkiel, S. P.; Miedaner, A.; Nozik, A. J. Growth of InP Nanostructures *via* Reaction of Indium Droplets with Phosphide Ions: Synthesis of InP Quantum Rods and InP-TiO_2 Composites. *J. Am. Chem. Soc.* **2004**, *126*, 2632–2639.
22. Pang, Q.; Zhao, L. J.; Cai, Y.; Nguyen, D. P.; Regnault, N.; Wang, N.; Yang, S. H.; Ge, W. K.; Ferreira, R.; Bastardaaa, G.; *et al.* CdSe Nano-Tetrapods: Controllable Synthesis, Structure Analysis, and Electronic and Optical Properties. *Chem. Mater.* **2005**, *17*, 5263–5267.
23. Larson, D. R.; Zipfel, W. R.; Williams, R. M.; Clark, S. W.; Bruchez, M. P.; Wise, F. W.; Webb, W. W. Water-Soluble Quantum Dots for Multiphoton Fluorescence Imaging *in Vivo*. *Science* **2003**, *300*, 1434–1436.
24. Olkhovets, A.; Hsu, R. C.; Lipovskii, A.; Wise, F. W. Size-Dependent Temperature Variation of the Energy Gap in Lead-Salt Quantum Dots. *Phys. Rev. Lett.* **1998**, *81*, 3539–3542.
25. Wise, F. W. Lead Salt Quantum Dots: The Limit of Strong Quantum Confinement. *Acc. Chem. Res.* **2000**, *33*, 773–780.
26. Narayanaswamy, A.; Feiner, L. F.; Meijerink, A.; van der Zaag, P. J. The Effect of Temperature and Dot Size on the Spectral Properties of Colloidal InP/ZnS Core−Shell Quantum Dots. *ACS Nano* **2009**, *3*, 2539–2546.
27. Chin, P. T. K.; de Mello Donegá, C.; van Bavel, S. S.; Meskers, S. C. J.; Sommerdijk, N. A. J. M.; Janssen, R. A. J. Highly Luminescent CdTe/CdSe Colloidal Heteronanocrystals with Temperature-Dependent Emission Color. *J. Am. Chem. Soc.* **2007**, *129*, 14880–14886.
28. Nonoguchi, Y.; Nakashima, T.; Kawai, T. Size- and Temperature-Dependent Emission Properties of Zinc-Blende CdTe Nanocrystals in Ionic Liquid. *J. Phys. Chem. C* **2007**, *111*, 11811–11815.
29. Schöps, O.; Le Thomas, N.; Woggon, U.; Artemyev, M. V. Recombination Dynamics of CdTe/CdS Core−Shell Nanocrystals. *J. Phys. Chem. B* **2006**, *110*, 2074–2079.
30. Klochikhin, A.; Reznitsky, A.; Dal Don, B.; Priller, H.; Kalt, H.; Klingshirn, C.; Permogorov, S.; Ivanov, S. Temperature Dependence of Photoluminescence Bands in $Zn_{1-x}Cd_xSe$/ZnSe Quantum Wells with Planar CdSe Islands. *Phys. Rev. B* **2004**, *69*, 085308.
31. Valerini, D.; Cretí, A.; Lomascolo, M.; Manna, L.; Cingolani, R.; Anni, M. Temperature Dependence of the Photoluminescence Properties of Colloidal CdSe/ZnS Core/Shell Quantum Dots Embedded in a Polystyrene Matrix. *Phys. Rev. B* **2005**, *71*, 235409.
32. Joshi, A.; Narsingi, K. Y.; Manasreh, M. O.; Davis, E. A.; Weaver, B. D. Temperature Dependence of the Band Gap of Colloidal CdSe/ZnS Core/Shell Nanocrystals Embedded into an Ultraviolet Curable Resin. *Appl. Phys. Lett.* **2006**, *89*, 131907.
33. Woo, J. Y.; Tripathy, S. K.; Kim, K.; Han, C. S. Thermal and Structural Dependence of the Band Gap of Quantum Dots Measured by a Transparent Film Heater. *Appl. Phys. Lett.* **2012**, *100*, 063105.
34. McLaurin, E. J.; Vlaskin, V. A.; Gamelin, D. R. Water-Soluble Dual-Emitting Nanocrystals for Ratiometric Optical Thermometry. *J. Am. Chem. Soc.* **2011**, *133*, 14978–14980.
35. Hsia, C. H.; Wuttig, A.; Yang, H. An Accessible Approach To Preparing Water-Soluble Mn^{2+}-Doped (CdSSe)ZnS (Core)Shell Nanocrystals for Ratiometric Temperature Sensing. *ACS Nano* **2011**, *5*, 9511–9522.
36. Maestro, L. M.; Rodríguez, E. M.; Rodríguez, F. S.; Iglesias-de la Cruz, M. C.; Juarranz, A.; Naccache, R.; Vetrone, F.; Jaque, D.; Capobianco, J. A.; Solé, J. G. CdSe Quantum Dots for Two-Photon Fluorescence Thermal Imaging. *Nano Lett.* **2010**, *10*, 5109–5115.
37. Yang, J.-M.; Yang, H.; Lin, L. W. Quantum Dot Nano Thermometers Reveal Heterogeneous Local Thermogenesis in Living Cells. *ACS Nano* **2011**, *5*, 5067–5071.
38. Choudhury, D.; Jaque, D.; Rodenas, A.; Ramsay, W. T.; Paterson, L.; Kar, A. K. Quantum Dot Enabled Thermal

Imaging of Optofluidic Devices. *Lab Chip* **2012**, *12*, 2414–2420.
39. Brites, C. D. S.; Lima, P. P.; Silva, N. J. O.; Millán, A.; Amaral, V. S.; Palacio, F.; Carlos, L. D. Thermometry at the Nanoscale. *Nanoscale* **2012**, *4*, 4799–4829.
40. Jaque, D.; Vetrone, F. Luminescence Nanothermometry. *Nanoscale* **2012**, *4*, 4301–4326.
41. Albers, A. E.; Chan, E. M.; McBride, P. M.; Ajo-Franklin, C. M.; Cohen, B. E.; Helms, B. A. Dual-Emitting Quantum Dot/Quantum Rod-Based Nanothermometers with Enhanced Response and Sensitivity in Live Cells. *J. Am. Chem. Soc.* **2012**, *134*, 9565–9568.
42. Okabe, K.; Inada, N.; Gota, C.; Harada, Y.; Funatsu, T.; Uchiyama, S. Intracellular Temperature Mapping with a Fluorescent Polymeric Thermometer and Fluorescence Lifetime Imaging Microscopy. *Nat. Commun.* **2012**, *3*, 705.
43. Maestro, L. M.; Jacinto, C.; Silva, U. R.; Vetrone, F.; Capobianco, J. A.; Jaque, D.; Solé, J. G. CdTe Quantum Dots as Nanothermometers: Towards Highly Sensitive Thermal Imaging. *Small* **2011**, *7*, 1774–1778.
44. Bao, H. B.; Gong, Y. J.; Li, Z.; Gao, M. Y. Enhancement Effect of Illumination on the Photoluminescence of Water-Soluble CdTe Nanocrystals: Toward Highly Fluorescent CdTe/CdS Core−Shell Structure. *Chem. Mater.* **2004**, *16*, 3853–3859.
45. Guo, J.; Yang, W. L.; Wang, C. C. Systematic Study of the Photoluminescence Dependence of Thiol-Capped CdTe Nanocrystals on the Reaction Conditions. *J. Phys. Chem. B* **2005**, *109*, 17467–17473.
46. Gaponik, N.; Talapin, D. V.; Rogach, A. L.; Hoppe, K.; Shevchenko, E. V.; Kornowski, A.; Eychmüller, A.; Weller, H. Thiol-Capping of CdTe Nanocrystals: An Alternative to Organometallic Synthetic Routes. *J. Phys. Chem. B* **2002**, *106*, 7177–7185.
47. Yu, W. W.; Peng, X. G. Formation of High-Quality CdS and Other II−VI Semiconductor Nanocrystals in Noncoordinating Solvents: Tunable Reactivity of Monomers. *Angew. Chem., Int. Ed.* **2002**, *41*, 2368–2371.
48. Pinna, N.; Weiss, K.; Urban, J.; Pileni, M. Triangular CdS Nanocrystals: Structural and Optical Studies. *Adv. Mater.* **2001**, *13*, 261–264.
49. Qian, H. F.; Dong, C. Q.; Weng, J. F.; Ren, J. C. Facile One-Pot Synthesis of Luminescent, Water-Soluble, and Biocompatible Glutathione-Coated CdTe Nanocrystals. *Small* **2006**, *2*, 747–751.
50. Sgobba, V.; Schulz-Drost, C.; Guldi, D. M. Synthesis and Characterization of Positively Capped CdTe Quantum Wires That Exhibit Strong Luminescence in Aqueous Media. *Chem. Commun.* **2007**, 565–567.
51. Zhou, Y. L.; Yang, M.; Sun, K.; Tang, Z. Y.; Kotov, N. A. Similar Topological Origin of Chiral Centers in Organic and Nanoscale Inorganic Structures: Effect of Stabilizer Chirality on Optical Isomerism and Growth of CdTe Nanocrystals. *J. Am. Chem. Soc.* **2010**, *132*, 6006–6013.
52. Li, Z. T.; Zhu, Z. N.; Liu, W. J.; Zhou, Y. L.; Han, B.; Gao, Y.; Tang, Z. Y. Reversible Plasmonic Circular Dichroism of Au Nanorod and DNA Assemblies. *J. Am. Chem. Soc.* **2012**, *134*, 3322–3325.
53. Li, Y. Y.; Zhou, Y. L.; Wang, H. Y.; Perrett, S.; Zhao, Y. L.; Tang, Z. Y.; Nie, G. J. Chirality of Glutathione Surface Coating Affects the Cytotoxicity of Quantum Dots. *Angew. Chem., Int. Ed.* **2011**, *50*, 5860–5864.
54. Betzel, C.; Saenger, W.; Hingerty, B. E.; Brown, G. M. Circular and Flip-Flop Hydrogen Bonding in β-Cyclodextrin Undecahydrate: A Neutron Diffraction Study. *J. Am. Chem. Soc.* **1984**, *106*, 7545–7557.
55. Wood, D. J.; Hruska, F. E.; Saenger, W. ^{1}H NMR Study of the Inclusion of Aromatic Molecules in α-Cyclodextrin. *J. Am. Chem. Soc.* **1977**, *99*, 1735–1740.
56. Lipkowitz, K. B. Applications of Computational Chemistry to the Study of Cyclodextrins. *Chem. Rev.* **1998**, *98*, 1829–1873.
57. Schneider, H.-J.; Hacket, F.; Rüdiger, V.; Ikeda, H. NMR Studies of Cyclodextrins and Cyclodextrin Complexes. *Chem. Rev.* **1998**, *98*, 1755–1785.
58. Kozár, T.; Venanzi, C. A. Reconsidering the Conformational Flexibility of β-Cyclodextrin. *J. Mol. Struct.* **1997**, *395−396*, 451–468.
59. Zhou, D.; Lin, M.; Chen, Z. L.; Sun, H. Z.; Zhang, H.; Sun, H. C.; Yang, B. Simple Synthesis of Highly Luminescent Water-Soluble CdTe Quantum Dots with Controllable Surface Functionality. *Chem. Mater.* **2011**, *23*, 4857–4862.
60. Liu, J.; Ong, W.; Román, E.; Lynn, M. J.; Kaifer, A. E. Cyclodextrin-Modified Gold Nanospheres. *Langmuir* **2000**, *16*, 3000–3002.
61. Varshni, Y. P. Temperature Dependence of the Energy Gap in Semiconductors. *Physica* **1967**, *34*, 149–154.
62. Wang, C. L.; Zhang, H.; Zhang, J. H.; Lv, N.; Li, M. J.; Sun, H. Z.; Yang, B. Ligand Dynamics of Aqueous CdTe Nanocrystals at Room Temperature. *J. Phys. Chem. C* **2008**, *112*, 6330–6336.
63. Sharma, R. C.; Chang, Y. A. The Cd-Te (Cadmium-Tellurium) System. *Bull. Alloy Phase Diagrams* **1989**, *10*, 334–339.
64. Adachi, S. *Handbook on Physical Properties of Semiconductors*; Springer: Berlin, 2004; Vol. 3.
65. Lee, K. M.; Wang, D. H.; Koerner, H.; Vaia, R. A.; Tan, L. S.; White, T. J. Enhancement of Photogenerated Mechanical Force in Azobenzene-Functionalized Polyimides. *Angew. Chem., Int. Ed.* **2012**, *51*, 4117–4121.
66. Murray, C. B.; Norris, D. J.; Bawendi, M. G. Synthesis and Characterization of Nearly Monodisperse CdE (E = S, Se, Te) Semiconductor Nanocrystallites. *J. Am. Chem. Soc.* **1993**, *115*, 8706–8715.
67. Peng, X. G. Green Chemical Approaches toward High-Quality Semiconductor Nanocrystals. *Chem.—Eur. J.* **2002**, *8*, 335–339.
68. Dai, Q. Q.; Zhang, Y.; Wang, Y. N.; Hu, M. Z.; Zou, B.; Wang, Y. D.; Yu, W. W. Size-Dependent Temperature Effects on PbSe Nanocrystals. *Langmuir* **2010**, *26*, 11435–11440.
69. Pradhan, N.; Battaglia, D. M.; Liu, Y. C.; Peng, X. G. Efficient, Stable, Small, and Water-Soluble Doped ZnSe Nanocrystal Emitters as Non-cadmium Biomedical Labels. *Nano Lett.* **2007**, *7*, 312–317.
70. Van de Broek, B.; Devoogdt, N.; D'Hollander, A.; Gijs, H. L.; Jans, K.; Lagae, L.; Muyldermans, S.; Maes, G.; Borghs, G. Specific Cell Targeting with Nanobody Conjugated Branched Gold Nanoparticles for Photothermal Therapy. *ACS Nano* **2011**, *5*, 4319–4328.
71. Maestro, L. M.; Haro-González, P.; Coello, J. G.; Jaque, D. Absorption Efficiency of Gold Nanorods Determined by Quantum Dot Fluorescence Thermometry. *Appl. Phys. Lett.* **2012**, *100*, 201110.
72. Shen, H. B.; Wang, H. Z.; Chen, X.; Niu, J. Z.; Xu, W. W.; Li, X. M.; Jiang, X.-D.; Du, Z. L.; Li, L. S. Size- and Shape-Controlled Synthesis of CdTe and PbTe Nanocrystals Using Tellurium Dioxide as the Tellurium Precursor. *Chem. Mater.* **2010**, *22*, 4756–4761.
73. Qu, L. H.; Peng, X. G. Control of Photoluminescence Properties of CdSe Nanocrystals in Growth. *J. Am. Chem. Soc.* **2002**, *124*, 2049–2055.
74. Nazzal, A. Y.; Wang, X. Y.; Qu, L. H.; Yu, W.; Wang, Y. J.; Peng, X. G.; Xiao, M. Environmental Effects on Photoluminescence of Highly Luminescent CdSe and CdSe/ZnS Core/Shell Nanocrystals in Polymer Thin Films. *J. Phys. Chem. B* **2004**, *108*, 5507–5515.